報 文
학학공학, 제10권 제3호
J. KIChE, Vol, 10, No. 3
June 1972.

工業用 粒子化플랜트의 시뮬레이션과 컨트롤

한 창 대*

Simulation and Control of Industrial Granulation Plants

*C. D. Han

Dept. of Chem. Eng., Polytechnic Institute of Brooklyn

Abstract

A first attempt is presented at investigating the problems of the automatic control of a diammonium phosphate granulation plant. This system is chosen for its simplicity, requiring one solid and one liquid feed stream to the granulator. A dynamic model is developed for the granulator in the form of a set of nonlinear differential equations in the zeroth, first and second moments of the granulator discharge stream particle size distribution. The equations are linearized and it is shown that the responses to similar disturbances of both the nonlinear and linear systems agree closely. Using the linear form, the model is extended to include the entire plant and a feedforward controller is designed by which disturbances in feed rate are used for manipulating the product recycle ratio to maintain constant the average particle size of granulator product.

1. Introduction

The granulation process is utilized in many fields where a particulate product of fairly narrow size range is required. Particle growth is carried out in a vessel called the granulator, and the particles may consist of more than one component, requiring several solid and liquid feed streams. Little work has been reported in the literature on the mathematical modelling of granulation plants, and the present paper is the second of two dealing with this topic. The first paper (2) dealt with the steady-state modelling of the granulator alone, and in this paper we extend the model to include the entire plant and investigate a method for controlling it. For a first study, we consider here the process for manufacturing diammonium phosphate, as developed by the Tennessee Valley Authority at Muscle Shoals, Alabama(4).

In the manufacture of diammonium phosphate granules, phosphoric acid (of approximately 75 % concentration) is reacted with ammonia vapor to produce a slurry of fine particles, a mixture of monoammonium and diammonium phosphates. This slurry is then pumped to an inclined rotating drum, the granulator, where it is sprayed on a tumbling bed of granules. Submerged in the granule bed is a perforated pipe through which ammonia is injected to complete the conversion of the slurry particles to diammonium phosphate.

The process is shown schematically in Fig. 1. Particles leaving the granulator are separated into

*Dept. of Chem. Eng., Polytechnic Institute of Brooklyn

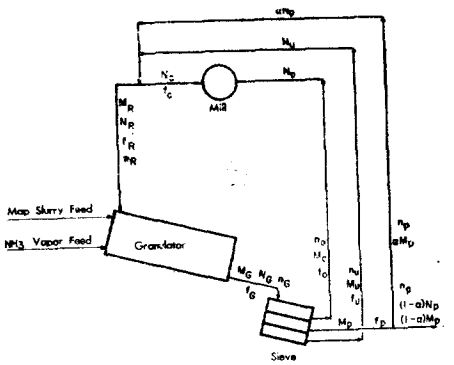

Fig. 1. Schematic of DAP Granulation Process.

three streams by the sieve, namely undersize, product-size and oversize. Part of the product-size stream is withdrawn as plant product and the rest is recycled, together with the undersize and, after crushing, the oversize. Since the two liquid streams feeding the granulator (slurry and ammonia) are controlled in a fixed-ratio, they can be considered as one. Hence in such diammonium phosphate (DAP) plants, the granulator has essentially one liquid and one solid feed stream, a configuration somewhat simpler than those for the granulation of mixed fertilizers, say.

In the previous paper (2) the authors described a steady-state model for a DAP granulator and tested it on data supplied by the TVA Pilot Plant at Muscle Shoals, Alabama. For the steady-state model, a number of assumptions were made:

a) The crusher is the source of new granules, i.e., no significant formation of new particles, (e.g., by attrition) takes place anywhere else in the plant.

b) Sieve efficiency is 100 %, i.e., the three streams, undersize, product-size and oversize are separated cleanly. Consider a typical particle size distribution function for the granulator discharge stream, as shown in Fig. 2. D_1 and D_4 are the smallest and largest particle sizes, respectively, and D_2 and D_3 are the lower and upper sieve apertures, respectively. Then we assume that no particles smaller than D_3 appear in the oversize and none smaller than D_2 appear in the product size.

c) The residence time of individual granules in the granulator is distributed probabilistically.

d) Granule growth rate is uniform, i.e., granules grow at the same rate independent of their size. This assumption accords with the growth mechanism which is believed to occur in this type of unit. In mixed fertilizer plants, particles can generally grow only by agglomeration. However, in DAP plants, particles grow by being wetted with slurry and contacted with ammonia. Each wetting and reaction lays down a layer of DAP, and a particle passing through the granulator will be subject to a number of such wettings in proportion to the time it spends in the granulator.

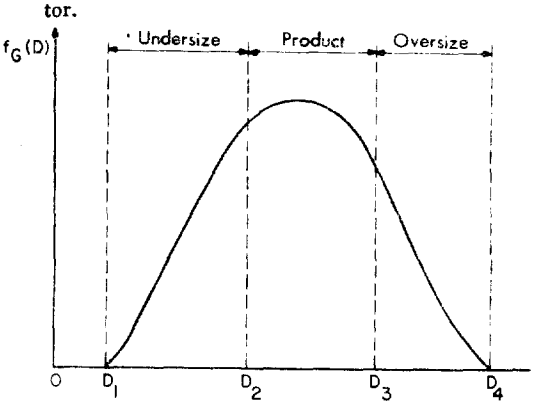

Fig. 2. Particle Size Distribution of Granulator Discharge Stream.

On the basis of these assumptions, Fig. 1 and 2 clearly show the relation of the recycle stream particle size distribution to that of the granulator discharge. Thus:

$$f_R(D)=\frac{1}{M_R}[M_G(D\,|\,D\leq D_2)+M_o f_C(D)+\alpha M_G f_G\,(D\,|\,D_2<D\leq D_3)] \quad (1)$$

where α is the product recycle fraction. By inserting plant data for the particle size distributions of the granulator discharge and the crusher discharge in Equation (1), a calculated recycle distribution was obtained. This was found to agree well with plant recycle data (2).

Then, using plant data for the granulator discharge particle size distribution and calculated values for the recycle distribution, a value of plant recycle ratio

was determined and this, too, was found to agree closely with plant data (2). Finally, by assuming a simple relationship between crusher speed and the particle size distribution of crusher product, it was shown that changes in recycle ratio had always to be made in conjunction with changes in crusher speed, if steady-state operation was to be maintained. This interdependence held regardless of the actual plant production rate.

For purposes of the steady-state study, the granulator alone was modelled. However, for a control study, the entire plant must be considered, and a more complete description follows.

2. Process Description

Fig. 3 is a simplified typical flow diagram of a granulator plant, designed largely to show the locations of plant transport lags. It is to be understood that Fig. 3 represents merely one of a large number of possible arrangements. Referring to the figure, process flow is as follows.

A stream of aqueous phosphoric acid is fed to the preneutralizer, into which is sparged a flow-controlled stream of ammonia vapor. The precipitate so formed is maintained in suspension and fed to the granulator. Submerged in the granule bed is a sparger through which additional ammonia is injected, thus depositing DAP on the recycled particles and increasing their size.

Moist granules are discharged from the granulator to the dryer, which is followed immediately by a cooler. The dryer and cooler are shown as one vessel for simplicity. Dry material from the dryer/cooler goes to the sieve, where it is separated into three fractions, oversize, undersize and product size, the last of which is continuously weighed.

The undersize material is deposited directly on the recycle belt conveyor. Oversize material passes through the crusher first, before going to the recycle conveyor. Product size material flows into the hopper of the product recycle feeder. The latter withdraws a controlled fraction of the product size and deposits that on the recycle conveyor. Whatever is not so withdrawn overflows the feeder hopper onto the product conveyor which removes it to storage as plant product. It is obvious that the product recycle fraction α is the ratio of the mass flow reading of the

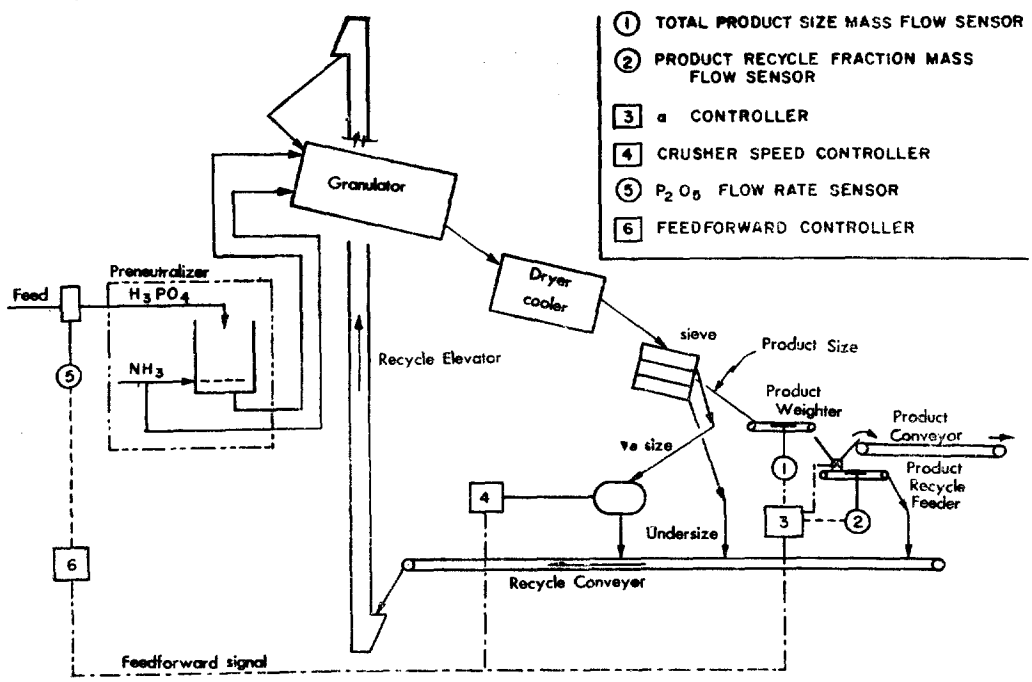

Fig. 3. Process Flow Schematic for DAP Granulation Plant.

product recycle feeder to that of the product weigher.

Finally, the recycle conveyor delivers the combined recycle stream to the recycle bucket elevator, which lifts it up to the granulator inlet.

Very little instrumentation is shown in Fig. 3 and something should be said about what is not shown. The two streams of ammonia vapor must be flow-ratio-controlled from the acid stream flow rate. Furthermore, the acid stream has two variables that must be monitored, concentration and flow rate, in order that the overall plant material balance on P_2O_5 be maintaied. Then, of course, the liquid level in the preneutralizer must be controlled by controlling the rate at which slurry is pumped to the granulator.

Apart from the selection of materials of construction to withstand this particular chemical system, the control techniques involved to carry out these functions represent no extrapolation of present technology.

Similarly, it is reasonable to assume that the dryer and cooler air flow rates, and dryer air inlet temperature have been well established to produce granules of the required dryness. In addition, there will be exhaust systems for the recovery of dust and vented ammonia, using recognized techniques.

Consequently, we exclude from this study all instrumentation associated with preneutralizing, drying, cooling and exhaust recovery. We concern ourselves only with a control system to determine product rate, maintain the product particle size distribution within the desired range and hold the granulation process in a stable state.

Clearly, the conveyor and elevator are simple transport delays. The dryer and cooler are usually of the rotating drum type. While the flow of solids through such equipment is never exactly plug flow, still, for simplicity, they too will be considered as transport delays. The sieve and crusher perform certain operations on the particle streams, but can be assumed to act instantaneously, so that any elapsed time can be lumped in with the other delays. Design of preneutralizers is commonly based on providing a certain hold-up time (3, 7). Hence the preneutralizer as well is a simple delay.

A logical schematic of the granulation plant can be constructed, showing how information on the significant plant parameters is transmitted from one piece of equipment to the other. This has been done in Fig. 4. Note that the feed is considered as being effectively a stream of DAP (in liquid form, say), delayed by the preneutralizer while en route to the granulator to be transformed into solid.

The box labelled "Sieve, Crusher and Product Recycle Feeder" is intended to show how the recycle stream is generated from the granulator product stream. In actual fact, the three separate functions included in the box are displaced from each other in time, but for purposes of this study we assume they are not, and that they take place instantaneously. Any elapsed time is included in the delay of the "Conveyor and Elevator."

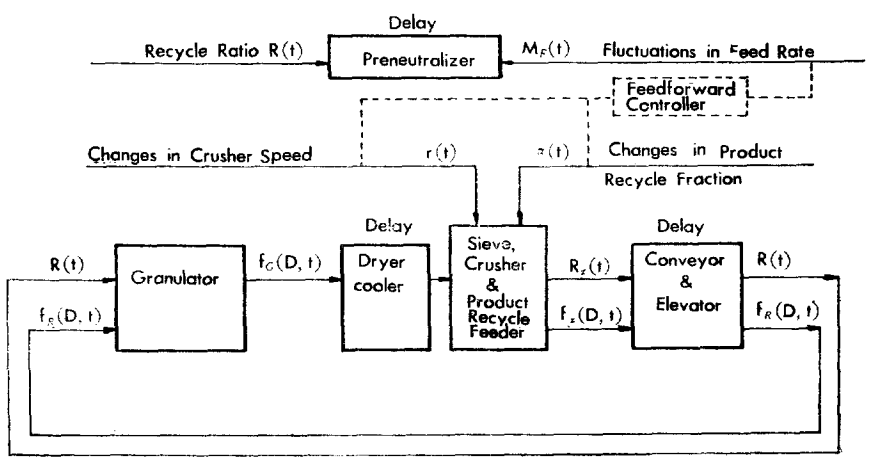

Fig. 4. Information Flow Schematic for DAP Granulation Plant.

The function $R(t)$ is the plant recycle ratio, defined as follows:

$$R(t)=\frac{M_R(t)}{M_F(t)} \qquad (2)$$

It must be clearly understood that $M_F(t)$ is the feed flow rate, not the product flow rate. Of course, at steady-state, they are equal. $R_X(t)$ and $f_X(D,t)$ are the values of the recycle ratio and the recycle size distribution prior to the delay of the "Conveyor and Elevator.".

When Fig. 4 is examined, it becomes obvious that feedforward control is needed. In processes with inherently long delays, measuring a disturbance in an output variable before taking corrective action means that such action would be too late to be effective. Instead, we monitor disturbances in an input variable and immediately take corrective action to prevent fluctuations in the output.

We see the essential control problem of the plant as one where we manipulate the product recycle ratio α (in combination with the crusher speed r) to return the plant to the steady-state after a disturbance in the effective DAP feed rate M_F.

3. Development of Mathematical Model

In modelling the DAP granulator in the steady-state, it was assumed that the residence time of particles in the granulator was probabilistically distributed (2). Preliminary work on the dynamic model showed that this assumption led to excessively difficult mathematics. The less stringent assumption was then made that particle residence time was uniform. However, this, too, led to considerable complexity.

The approach finally adopted for modelling the granulator in the dynamic state is shown diagrammatically in Fig. 5. It is now visualized as a two-compartment vessel. The first compartment, the Reaction Stage, is the one in which all particle growth is assumed to occur, and it is a well-mixed vessel so that the particle size distribution of its contents is the same as that of its discharge stream. The second compartment is the Drying Stage, in which no particle size change takes place. It is a plug flow vessel and represents a transport delay. If this delay is τ, then, using the nomenclature of Fig. 5,

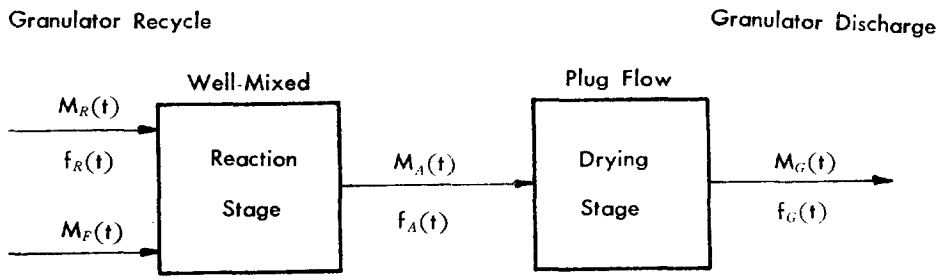

Fig. 5. Dynamic Model of DAP Granulator.

$$f_G(D,t)=f_A(D,t-\tau) \qquad (3)$$

where $f_A(D,t)$ is the particle size of the hypothetical stream leaving the Reaction Stage.

In actual fact, such an arrangement is not entirely hypothetical, since in some plants (3, 5) the slurry and ammonia spargers do not extend the full length of the granulator. Furthermore, in other plants (4), two separate vessels are employed. The first is the ammoniator and the second is a similar rotating drum, but without any heating or cooling facilities, merely providing residence time for the particles to "mature", as it were.

From this point on, the mathematical development will apply solely to the Reaction Stage, it being always understood that a transport delay τ must be appended in order to complete the granulator model. Recalling that the basic assumption in this study is that no particles are created outside the crusher, take a particle balance around the Reaction Stage. This will

be on particles of size D, from time t to time $(t+\Delta t)$. Applying the particle conservation law around the Reaction Stage, one has:

$$\Delta t[M_R(t)f_R(D,t)-M_A(t)-M_A(t)f_A(D,t)]+\Phi(t)[f_A(D-\Delta D,t)-f_A(D,t)]=[\Phi(t+\Delta t)f_A(D,t+\Delta t)-\Phi(t)f_A(D,t)] \quad (4)$$

Assuming that particles grow at the rate of ε mm./hr., the change in diameter in time t is given by

$$\Delta D=\varepsilon\,\Delta t \quad (5)$$

Substituting Equation (5) into Equation (4) and taking the limit, we obtain the differential particle balance:

$$\frac{\partial}{\partial t}[\Phi(t)f_A(D,t)]+\varepsilon\frac{\partial}{\partial D}[\Phi(t)f_A(D,t)]=M_R(t)f_R(D,t)-M_A(t)f_A(D,t) \quad (6)$$

Rewriting the left-hand side of Equation (6), we have

$$\Phi(t)\frac{\partial}{\partial t}f_A(D,t)+f_A(D,t)\frac{d}{dt}\Phi(t)+\varepsilon\,\Phi(t)\frac{\partial}{\partial D}f_A(D,t)=M_R(t)f_R(D,t)-M_A(t)f_A(D,t) \quad (7)$$

A differential mass balance about the ammoniator gives:

$$\frac{d}{dt}\Phi(t)=M_F(t)+M_R(t)-M_A(t) \quad (8)$$

Substituting Equation (8) into Equation (7), and simplifying:

$$\Phi(t)\frac{\partial}{\partial t}f_A(D,t)=-\varepsilon\,\Phi(t)\frac{\partial}{\partial D}f_A(D,t)+M_R(t)f_R(D,t)-[M_R(t)+M_F(t)]f_A(D,t) \quad (9)$$

We have here an equation in two independent variables, D and t. The dependence on D can be eliminated by taking moments. The n^{th} moment, μ_n, of a distribution function, $f(D)$, is defined by

$$\mu_n=\int_{all\ D}D^n f(D)dD$$

Thus, by multiplying both sides of Equation (9) by D^n and integrating with respect to size D over the entire size range, we obtain

$$\Phi(t)\frac{d}{dt}\mu_{An}(t)=n\,\varepsilon\,\Phi(t)\mu_{A\ n-1}(t)+M_R(t)\mu_{Rn}(t)-[M_R(t)+M_F(t)]\mu_{An}(t) \quad (10)$$

Assigning values of 0, 1, 2 and 3 to n in turn, we obtain four equations which define the dynamic behavior of the Reaction Stage product's particle size distribution moments in response to perturbations in feed rate, recycle rate and recycle particle size distribution. The four equations correspond, in turn, to the number of particles per unit mass of the product stream, and measures of particle size, surface and mass.

Therefore, it follows from Equation (10),

For $n=0$:

$$\phi(t)\frac{d}{dt}\mu_{A_0}(t)=M_R(t)\mu_{R_0}(t)-[M_R(t)+M_F(t)]\mu_{A_0}(t) \quad (11)$$

For $n=1$:

$$\phi(t)\frac{d}{dt}\mu_{A_1}(t)=\varepsilon\,\Phi(t)\mu_{A_0}(t)+M_R(t)\mu_{R_1}(t)-[M_R(t)+M_F(t)]\mu_{A_1}(t) \quad (12)$$

For $n=2$:

$$\Phi(t)\frac{d}{dt}\mu_{A_2}(t)=2\varepsilon\,\Phi(t)\mu_{A_1}(t)+M_R(t)\mu_{R_2}(t)-[M_R(t)+M_F(t)]\mu_{A_2}(t) \quad (13)$$

For $n=3$:

$$\Phi(t)\frac{d}{dt}\mu_{A_3}(t)=3\varepsilon\,\Phi(t)\mu_{A_2}(t)+M_R(t)\mu_{R_3}(t)-[M_R(t)+M_F(t)]\mu_{A_3}(t) \quad (14)$$

The last equation is a special case because of the definition of f(D). This is:

$$f(\mathrm{D})dD=\frac{\text{No. of particles in size range D to}(D+dD)}{\text{unit mass of particle stream}}$$

Hence, the third moment of $f(\mathrm{D})$ is a measure of the volume per unit mass. If multiplied by the particle volume shape factor and particle material density it becomes the mass per unit mass, i.e., unity. This will hold for all streams. Thus:

$$\nu\rho\mu_3(t)=1 \quad (15)$$

or

$$\mu_{A3}(t)=\mu_{R3}(t)=\frac{1}{\nu\rho} \quad (16)$$

and

$$\frac{d}{dt}\mu_{A3}(t)=0 \quad (17)$$

Substituting Equations (16) and (17) into Equation (14) yields:

$$M_F(t)=\Phi(t)\ 3\epsilon\ \nu\rho\mu_{A2}(t) \tag{18}$$

$\mu_{A2}(t)$ is a measure of the particle diameter squared, per unit mass, and the right-hand side of Equation (18) defines the total mass deposited per unit time in the reaction stage. This is seen to equal the feed rate $M_F(t)$. To continue the mathematical development, divide Equations (11), (12) and (13) by $\Phi(t)$, substitute from Equation (18) and rearrange. We obtain:

$$\frac{d\mu_{A_0}(t)}{dt}=3\epsilon\nu\rho\mu_{A_2}(t)[R(t)\mu_{R_0}(t)-(R(t)+1)\mu_{A_0}(t)] \tag{19}$$

$$\frac{d\mu_{A_1}(t)}{dt}=\epsilon\mu_{A_0}(t)+3\epsilon\nu\rho\mu_{A_2}(t)[R(t)\mu_{R_1}(t)-(R(t)+1)\mu_{A_1}(t)] \tag{20}$$

$$\frac{d\mu_{A_2}(t)}{dt}=2\epsilon\mu_{A_1}(t)+3\epsilon\nu\mu_{A_2}(t)[R(t)\mu_{R_2}(t)-(R(t)+1)\mu_{A_2}(t)] \tag{21}$$

Where $R(t)=\dfrac{M_R(t)}{M_F(t)}$ is the recycle ratio.

Equations (19), (20) and (21) describe the dynamic response of μ_{A_0}, μ_{A_1} and μ_{A_2} to forcing functions R, μ_{R_0}, μ_{R_2}. It is to be noted that dependence on actual flow rates is eliminated.

These equations are therefore the model of the dynamic behavior of the Reaction Stage.

By setting the left-hand sides of Equations (19)-(21) to zero, we can obtain steady-state relationships for the model. From Equation (19):

$$\bar{R}\bar{\mu}_{R_0}=(\bar{R}+1)\bar{\mu}_{A_0} \tag{22}$$

This equation is a statement that the number of particles entering the Reaction Stage per unit time equals the number leaving. We thus verify that one of our basic assumptions has been maintained. From Equation (20):

$$\epsilon\bar{\mu}_{A_0}+3\epsilon\nu\rho\bar{\mu}_{A_2}[\bar{R}\bar{\mu}_{R_1}-(\bar{R}+1)\bar{\mu}_{A_1}]=0 \tag{23}$$

From Equation (21):

$$2\epsilon\bar{\mu}_{A_0}+3\epsilon\nu\rho\bar{\mu}_{A_2}[\bar{R}\mu_{R_2}-(\bar{R}+1)\bar{\mu}_{A_2}]=0 \tag{24}$$

Defining the following deviation variables:

$$\begin{aligned}\Delta\mu_{Rn}(t)&=\bar{\mu}_{Rn}-\bar{\mu}_{Rn}(t)\\ \Delta R(t)&=\bar{R}-R(t)\\ \Delta\mu_{An}(t)&=\bar{\mu}_{An}-\mu_{An}(t)\end{aligned} \tag{25}$$

in which the barred terms are the steady-state values. Substituting into Equations (19)-(21) from Equations (25), and neglecting all those terms which are higher than the first order in deviation variables, we obtain:

$$\frac{d}{dt}\Delta\mu_{A_0}=-C_1\Delta\mu_{A_0}+C_2\Delta R+C_3\Delta\mu_{R_0} \tag{26}$$

$$\frac{d}{dt}\Delta\mu_{A_1}=C_4\Delta\mu_{A_0}-C_1\Delta\mu_{A_1}-C_5\Delta\mu_{A_2}+C_6\Delta R+C_3\Delta\mu_{R_1} \tag{27}$$

$$\frac{d}{dt}\Delta\mu_{A_2}=C_7\Delta\mu_{A_1}-C_8\Delta\mu_{A_2}+C_9\Delta R+C_3\Delta\mu_{R_2} \tag{28}$$

Where the coefficients C_i are as listed in Table I.

Table 1. Coefficient Array for the Linearized Reaction Stage Equations

$C_1=3\ \epsilon\ \nu\ \rho\ \bar{\mu}_{A_2}(\bar{R}+1)$	$=3.581874$
$C_2=3\ \epsilon\ \nu\ \rho\ \bar{\mu}_{A_2}(\bar{\mu}_{R_0}-\bar{\mu}_{A_0})$	$=215,267$
$C_3=3\ \epsilon\ \nu\rho\ \bar{\mu}_{A_2}\bar{R}$	$=2.718772$
$C_4=\epsilon$	$=0.4$
$C_5=3\ \epsilon\ \nu\rho\ [(\bar{R}+1)\bar{\mu}_{A_1}-\bar{R}\bar{\mu}_{R_1}]$	$=0.370383$
$C_6=3\ \epsilon\ \nu\rho\ \bar{\mu}_{A_2}(\bar{\mu}_{R_1}-\bar{\mu}_{A_1})$	$=102405$
$C_7=2\ \epsilon$	$=0.8$
$C_8=3\ \epsilon\ \nu\rho\ [2(\bar{R}+1)\bar{\mu}_{A_2}-\bar{R}\bar{\mu}_{R_2}]$	$=4.277570$
$C_9=3\ \epsilon\ \nu\rho\ \bar{\mu}_{A_2}(\bar{\mu}_{R_2}-\bar{\mu}_{A_2})$	$=45092$

4. Simulation of the Granulation Plant

4.1. Simulation of the Reaction Stage

Equations (26), (27) and (28) are a set of linear differential equations, in which the $\Delta\mu_{An}$ are response variables and ΔR and the $\Delta\mu_{Rn}$ are forcing variables. We wish to see how the $\Delta\mu_{An}$ respond to disturbances, which, for the purposes of this study, will always be step changes. Thus, at steady-state, ΔR and the $\Delta\mu_{Rn}$ will all be zero, and at non steady-state, ΔR and the $\Delta\mu_{Rn}$ will have certain fixed values.

Disturbances can occur in feed rate, product recycle fraction and crusher speed, their magnitudes being δM_F, $\delta\alpha$ and δr, respectively. These represent frac-

tional changes from certain steady-state values as identified by the reference Run No. 11 in the previous paper (2).

Using any particular value of δM_F, $\delta\alpha$ and δr, the step changes ΔR and $\Delta\mu_{Rn}$ can be computed (7). Changes in crusher speed are assumed never to occur alone, but always in conjunction with changes in product recycle fraction. The relation between magnitudes of δr and $\delta\alpha$ is determined by the steady-state operating line (2).

In summary, values of ΔR and the $\Delta\mu_{Rn}$ were computed for eighteen different disturbances, namely:

(i) Feed rate $\delta M_F = \pm 0.01, \pm 0.05, \pm 0.10$.

(ii) Product recycle fraction $\delta\alpha = \pm 0.01, \pm 0.05, \pm 0.10$.

(iii) α with crusher speed $\delta\alpha = \pm 0.01, \pm 0.05, \pm 0.10$.

The eighteen sets of conditions were fed into an analog computer program set up for Equations (26), (27) and (28), and the responses of the $\Delta\mu_{An}$ were plotted. Figures 6, 7 and 8 are selected outputs of the analog progrm. Figure 6 shows the responses of the $\Delta\mu_{An}$ to fractional step increases in α of 0.01,

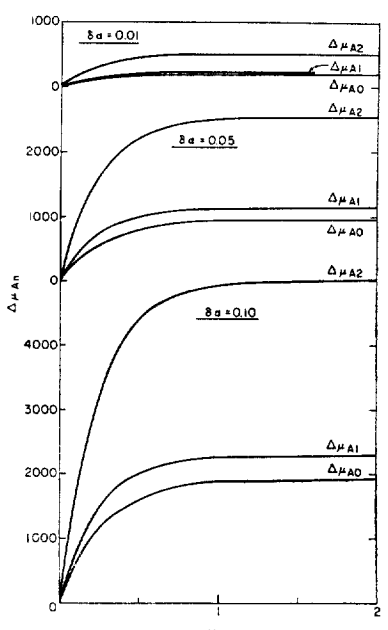

Fig. 6. Response to Disturbances of Linearized Reaction Stage Changes in α.

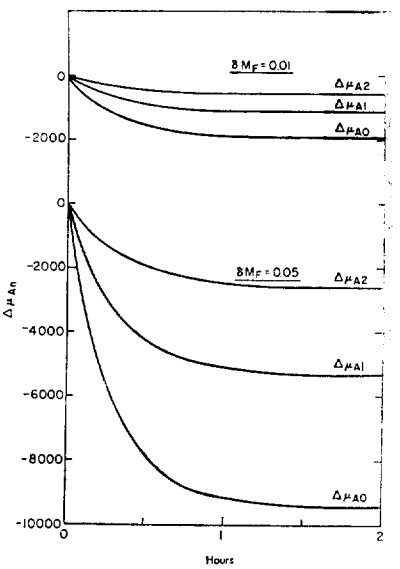

Fig. 7. Response to Disturbances of Linearized Reaction Stage Changes in MF.

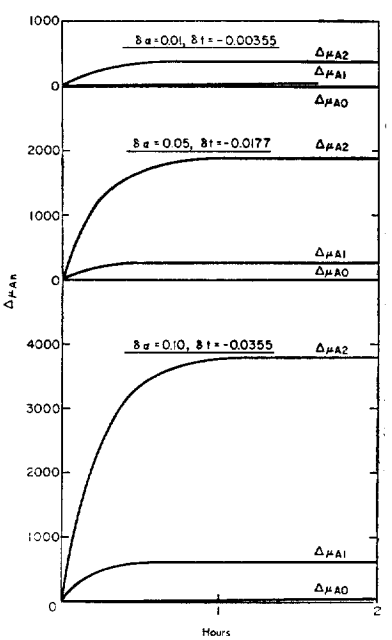

Fig. 8. Response to Disturbances of Linearized Reaction Stage Changes in α with r.

0.05 and 0.10. Fig. 7 shows the responses to fractional step increases in M_F of 0.01 and 0.05. Fig. 8 shows the responses to the same disturbances when α and r are changed together.

It is desirable, of course, to check how well the linearized system represents the original nonlinear system. In other words, how closely does the dynamic response of the linearized Equations (26), (27) and (28) approach the dynamic response of the nonlinear Equations (19), (20) and (21)?

To this end, the latter set of equations was integrated by a Runge-Kutte predictor-corrector method, for the same eighteen different disturbances as before. This required the prior calculation of perturbed values for the forcing variables R and the μ_{Rn}, and the incorporation of these perturbed values in the equation coefficients (6). The results confirmed that the use of the linearized equations is reasonably good for disturbances as high as 10%. Furthermore, the model's behavior is readily explicable.

We also note that in the cases in which the product recycle fraction α changes together with crusher speed r, the response of $\Delta\mu_{A_1}$ and $\Delta\mu_{A_2}$ are less than they would be for α alone. The inference is that whereas an increase in α would increase the recycle flow rate, the corresponding reduction in r decreases the number of particles leaving the crusher, and these two changes in particle flow rate balance in such a way that the number of particles per unit mass of Reaction Stage discharge is kept constant. This result points up the validity of the Steady-state operating line.

4.2. Simulation of the Complete Plant

Fig. 4 is an information flow schematic for the DAP Granulation Plant. A linearized version of this diagram can be drawn, showing, in addition, the finally adopted model of the granulator, and the response and forcing variables in more detail. This has been done in Fig. 9, and the following explanatory notes apply:

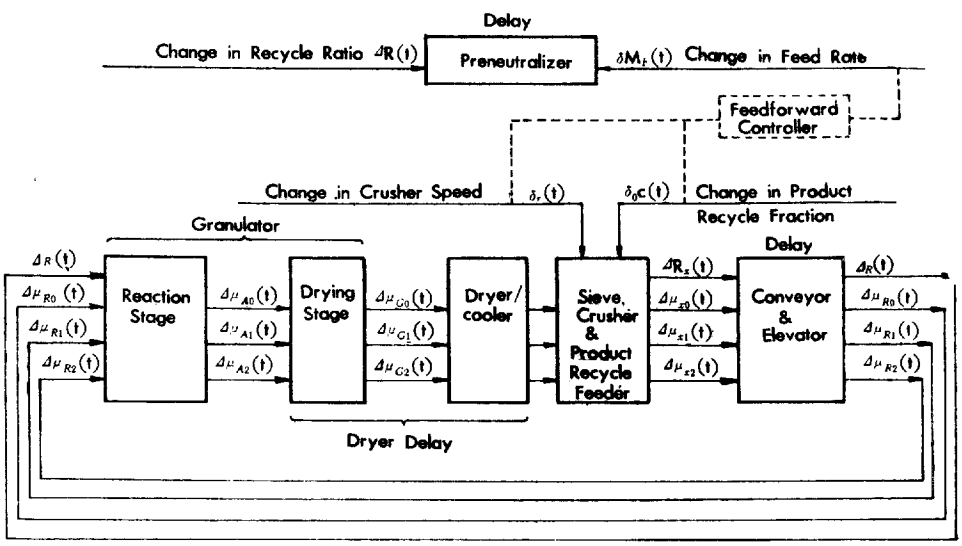

Fig. 9. Information Flow Schematic of Linearized Plant.

If the feed rate increases, but the recycle rate is fixed, the same number of particles have more material available for growth. The discharge stream becomes coarser, there are fewer particles per unit mass, and $\Delta\mu_{A_0}$ is negative. If the feed rate is fixed and the recycle rate increases (because of an increase in α), the reverse happens.

i) As discussed previously, the feed to the plant consists actually of two streams, phosphoric acid and ammonia. However, for simplicity, they are considered as combined effectively in one feed stream of diammonium phosphate.

ii) The preneutralizer is considered to be a simple delay.

iii) For a fractional change δM_F in feed rate, the perturbation in plant recycle ratio R is given by

$$\Delta R = -\bar{R}\ \delta\ M_F \qquad (29)$$

iv) The Reaction Stage has already been simulated on the analog computer. However, the forcing variables ΔR and $\Delta\mu_{Rn}$ were then incorporated as input voltages, and now they are to be fed in from another part of the system.

v) The delay of the Granulator Drying Stage is lumped together with that for the dryer, proper. For the analog model, each of the three $\Delta\mu_{Rn}$ must be connected to identical delay circuits.

vi) The $\Delta\mu_{Gn}$ are shown as inputs to the block labelled "Sieve, Crusher and Product Recycle Feeder." In this block we generate the ΔR_x and $\Delta\mu_{xn}$ as functions of $\delta\alpha$ and δr. They are the forcing functions for the Granulator Reaction Stage, ΔR and $\Delta\mu_{Rn}$, prior to the transport delay of the Recycle Conveyor and Elevator.

We quote here (6) the relations required for computing ΔR_x for a given $\delta\alpha$, and the $\Delta\mu_{xn}$ for a given $\delta\alpha$ with and without δr:

$$\Delta R_x = \frac{\bar{\alpha}\,\delta\alpha}{1-\bar{\alpha}} \qquad (30)$$

For change in α alone:

$$\left.\begin{aligned}\Delta\mu_{x_0} &= (-24120 + 0.032124\,\Delta\mu_{G_0})\delta\alpha\\ \Delta\mu_{x_1} &= (10841 + 0.070047\,\Delta\mu_{G_1})\delta\alpha\\ \Delta\mu_{x_2} &= (65804 + 0.128176\,\Delta\mu_{G_2})\delta\alpha\end{aligned}\right\} \qquad (31)$$

For change in α with r:

$$\left.\begin{aligned}\Delta\mu_{x_0} &= (-50146 + 0.032124\,\Delta\mu_{G_0})\delta\alpha\\ \Delta\mu_{x_1} &= (-10545 + 0.070047\,\Delta\mu_{G_1})\delta\alpha\\ \Delta\mu_{x_2} &= (50028 + 0.128176\,\Delta\mu_{G_2})\delta\alpha\end{aligned}\right\} \qquad (32)$$

When actual values of the $\Delta\mu_{Gn}$ are inserted in Equations (31) and (32), however, the second terms on the right-hand sides turn out to be very small compared to the first terms. When it comes to inserting them in the analog model, they are too small to be accommodated by pot settings, at least on the EAI TR 48 units employed.

Hence, whereas the actual process has a closed loop, the analog simulation, owing to the limitations of the equipment, does not. Equations (31) and (32) can be simplified.

For change in α alone:

$$\left.\begin{aligned}\Delta\mu_{x_0} &= -24120\,\delta\alpha\\ \Delta\mu_{x_1} &= 10841\,\delta\alpha\\ \Delta\mu_{x_2} &= 65802\,\delta\alpha\end{aligned}\right\} \qquad (33)$$

For change in α with r:

$$\left.\begin{aligned}\Delta\mu_{x_0} &= -50146\,\delta\alpha\\ \Delta\mu_{x_1} &= -10545\,\delta\alpha\\ \Delta\mu_{x_2} &= 50028\,\delta\alpha\end{aligned}\right\} \qquad (34)$$

vii) To represent the conveyor and elevator, each of the four functions, ΔR_{x_1}, $\Delta\mu_{x_0}$, $\Delta\mu_{x_1}$ and $\Delta\mu_{x_2}$ must be connected to four identical delay circuits. heT four outputs from these delays are the forcing functions ΔR and $\Delta\mu_{Rn}$, which are fed as inputs to the Granulator Reaction Stage. In addition, the ΔR function obtained from this source is summed to that obtained for a change in M_F.

With the above points in mind, an analog diagram for the complete Granulation Plant was prepared. The pot settings in the delay circuits provide the following delays:

Preneutralizer	60 mins (Computer time 60 secs)
Elevator and Conveyor	30 mins (Computer time 30 secs)
Dryer(with Granulator Drying Section)	80 mins (Computer time 80 secs)

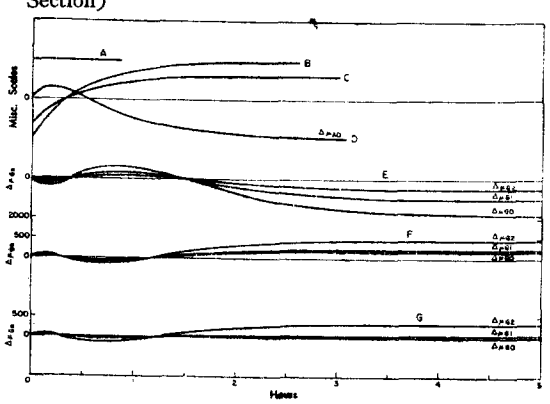

Fig. 10. Various Outputs from Granulation Plant Analog Simulation.

Fig. 10 shows a series of automatically plotted outputs obtained from the plant model. They are labelled A through G, and are commented on below

in sequence:

i) Trace A is the initial positive step input of the computer variable $[100\,\delta M_F]$, which corresponds to the plant variable δM_F. The magnitude of the disturbance shown is equivalent to a 1.0 % step increase in feed rate.

ii) Trace B is the step increase in feed rate delayed one hour by the preneutralizer. It is at once apparent that the first-order Padé approximation used is a rather poor representation of a delay. The worst défect is the large negative "spike" from time zero to one-third of the nominal delay. A second defect is that, when the nominal delay time has elapsed, the magnitude of the signal is only 71 % of the input value.

iii) Trace C is that of the computer variable $+[20(-\Delta R)]$ which results from the delayed $+[100\delta M_F]$. It has the same general form as trace B, but differs in magnitude. It seems clear that if trace B had been an accurate step, trace C would have been one also.

iv) Trace D is taken at the Reaction Stage outlet. It corresponds to the zeroth moment of the Reaction Stage discharge particle size distribution, represented by the computer variable $+\left[\frac{\Delta\mu_{A0}}{2000}\right]$. This curve exhibits an initial small positive portion, followed by a smoothly increasing negative portion, which eventually settles down to a steady value, about 3 hours after the initial disturbance and 2 hours after the delayed disturbance.

The positive loop is obviously caused by the false negative spike of the first-order Padé approximation. The remainder of the curve indicates that, without that negative spike, the response would have agreed closely with the one obtained in the previous section.

v) Traces E are those of the computer variables corresponding to the zeroth, first and second moments of the dryer discharge particle size distribution, i.e., delayed 80 minutes beyond trace D. Thus a second poor delay approximation has been superimposed on the first, giving rise to the fluctuations shown. The true curves really begin after a time of 2.33 hours. They are smooth, increasingly negative, and reach steady-state after about 4.33 hours, or 2.0 hours beyond the total time delay. Comparison with the curves obtained in the previous section shows close agreement.

vi) Traces F correspond to traces E, except that instead of a step increase in feed rate of 1.0 %, the disturbance is a 1.0 % step increase in the produce recycle fraction α.

The identical comments apply as for the E traces. Initial fluctuations are due solely to poor approximations to delays, and the latter part of the curves agree closely with those obtained in the previous section.

vii) Traces G are the same variables, responding now to a 1.0 % step increase in α, combined with a corresponding step change in crusher speed r. Comments are as for the previous.

5. Control of the Plant

5. 1. Design of Feedforward Controller

Consider the linearized model of the Granulator Reaction Stage, as defined in Equations (26), (27) and (28). We have here four input variables, ΔR and the three $\Delta\mu_{Rn}$. In the granulation plant, we consider the feed rate to be the input disturbance, or rather (in the linearized model) the corresponding deviation variable δM_F. Furthermore, the manipulative variable available to us is the product recycle fraction, and again we use the corresponding deviation variable $\delta\alpha$. Note that neither δM_F nor $\delta\alpha$ appear in Equations (26)-(28), explicitly. But we know, from Equations (29), (30), (33) and (34) that changes in M_F result in changes in R, and changes in α result in changes in R and in the μ_{Rn}. However, in order to substitute for the ΔR and $\Delta\mu_{Rn}$ as they appear in Equations (26)-(28) in terms of δM_F and $\delta\alpha$, we must take into account the time displacements caused by the system delays.

Time relationships are illustrated in Fig. 11, based on time t measured at the outlet of the Granulator Reaction Stage.

At time t, any change in recycle ratio R occurring at the Reaction Stage is due to one of two causes.

a) A disturbance in feed rate M_F occurring at time $(t-T_1)$, i.e., prior to the preneutralizer, or

b) A change in product recycle fraction α(with or

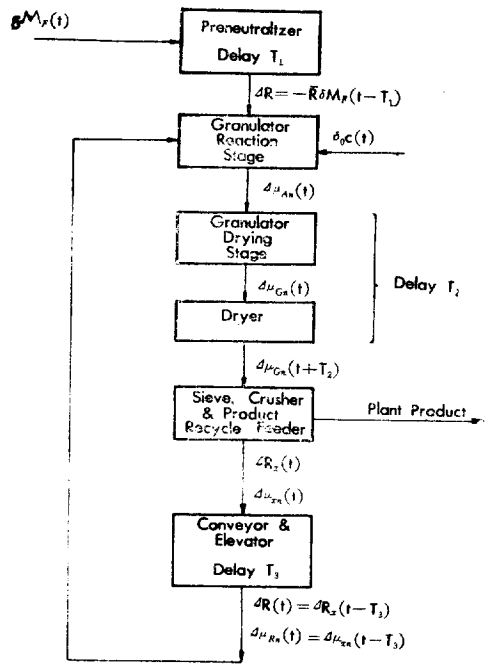

Fig. 11. DAP Granulation Plant Schematic Showing Time Relationships.

without a change in crusher speed r) occurring at time $(t-T_3)$, i.e., prior to the conveyor and elevator.

Furthermore, at time t, any change in recycle size distribution moments occurring at the Reaction Stage is due to cause b), above.

Taking the time relationships into account, we rewrite Equation (29) thus:

$$\Delta R(t) = -\bar{R}\delta M_F(t-T_1) \tag{35}$$

and Equation (30) thus:

$$\Delta R(t) = \frac{\bar{\alpha}}{1-\bar{\alpha}}\delta\alpha(t-T_3) = \bar{A}\delta\alpha(t-T_3) \tag{36}$$

Of course, the total change in recycle ratio is the sum of the two terms.

$$\Delta R(t) = \bar{A}\delta\alpha(t-T_3) - \bar{R}\delta M_F(t-T_1) \tag{37}$$

Similarly, we rewrite Equations (33) and (34) thus: For change in α alone:

$$\begin{aligned}\Delta\mu_{R_0} &= -24120\,\delta\alpha(t-T_3) = P_0\,\delta\alpha(t-T_3)\\ \Delta\mu_{R_1} &= 10841\,\delta\alpha(t-T_3) = P_1\,\delta\alpha(t-T_3)\\ \Delta\mu_{R_2} &= 65802\,\delta\alpha(t-T_3) = P_2\,\delta\alpha(t-T_3)\end{aligned} \tag{38}$$

For change in both α and r:

$$\begin{aligned}\Delta\mu_{R_0} &= -50146\,\delta\alpha(t-T_3) = Q_0\,\delta\alpha(t-T_2)\\ \Delta\mu_{R_1} &= -10545\,\delta\alpha(t-T_3) = Q_1\,\delta\alpha(t-T_3)\\ \Delta\mu_{R_2} &= 50028\,\delta\alpha(t-T_3) = Q_2\,\delta\alpha(t-T_3)\end{aligned} \tag{39}$$

Assume for the moment that we manipulate α alone. Substituting into Equations (26), (27) and (28) from Equations (37) and (38), we get:

$$\begin{aligned}\frac{d}{dt}\Delta\mu_{A_0}(t) = &-C_1\Delta\mu_{A_0}(t) + C_2\bar{A}\delta\alpha(t-T_3)\\ &-C_2\bar{R}\delta M_F(t-T_1) + C_3P_0\delta\alpha(t-T_3)\end{aligned} \tag{40}$$

$$\begin{aligned}\frac{d}{dt}\Delta\mu_{A_1}(t) = &C_4\Delta\mu_{A_0}(t) - C_1\Delta\mu_{A_1}(t) - C_5\,\Delta\mu_{A_2}(t)\\ &+C_6\bar{A}\delta\alpha(t-T_3) - C_6\bar{R}\delta M_F(t-T_1)\\ &+C_3P_1\delta\alpha(t-T_3)\end{aligned} \tag{41}$$

$$\begin{aligned}\frac{d}{dt}\Delta\mu_{A_2}(t) = &C_7\Delta\mu_{A_1}(t) - C_8\Delta\mu_{A_2}(t) + C_9\bar{A}\delta\alpha(t-T_3)\\ &-C_9\bar{R}\delta M_F(t-T_1) + C_3P_2\delta\alpha(t-T_3)\end{aligned} \tag{42}$$

The equations now contain one input disturbance variable δM_F and one manipulative variable $\delta\alpha$. With one manipulative variable, we can have only one controlled variable (1), and we are faced with choosing one of the $\Delta\mu_{An}$. What this means is that, while ideally we could wish that all three were maintained at zero, we must actually be satisfied with keeping one of them zero and letting the other two "float" where they will.

Since we are primarily interested in maintaining the size range of the granulator product stream constant, it makes sense to pick $\Delta\mu_{A_1}(t)$ for the controlled variable. The first moment of a particle size distribution is a measure of its average size. Set the left-hand side of Equation (41) to zero, and make $\Delta\mu_{A_1}(t)$ zero in all three Equations (40), (41) and (42), thus:

$$\begin{aligned}\frac{d}{dt}\Delta\mu_{A_0}(t) = &-C_1\Delta\mu_{A_0}(t) + C_2\bar{A}\delta\alpha(t-T_3)\\ &-C_2\bar{R}\delta M_F(t-T_1) + C_3P_0\delta\alpha(t-T_3)\end{aligned} \tag{43}$$

$$\begin{aligned}0 = &C_4\Delta\mu_{A_0}(t) - C_5\Delta\mu_{A_2}(t) + C_6\bar{A}\delta\alpha(t-T_3)\\ &-C_6\bar{R}\delta M_F(t-T_1) + C_3P_1\delta\alpha(t-T_3)\end{aligned} \tag{44}$$

$$\frac{d}{dt}\Delta\mu_{A_2}(t)=-C_8\Delta\mu_{A_2}(t)+C_9\bar{A}\delta\alpha(t-T_3)$$
$$-C_9\bar{R}\delta M_F(t-T_1)+C_3P_2\delta\alpha(t-T_3) \quad (45)$$

Here are three equations containing four variables, namely $\Delta\mu_{A_0}$, $\Delta\mu_{A_2}$, δM_F and $\delta\alpha$. By eliminating $\Delta\mu_{A_0}$ aud $\Delta\mu_{A_2}$, we can obtain $\delta\alpha$ as a function of δM_F, and by the use of Laplace transforms, we can obtain an expression, in the complex plane, for the transfer function $\frac{d\alpha(s)}{dM_F(s)}$, where $d\alpha(s)$ aud $dM_F(s)$ are the Laplace transforms of $\delta\alpha(t)$ and $\delta M_F(t)$ respectively. The transfer function $\frac{d\alpha(s)}{dM_V(s)}$ relates the manipulative variable $\delta\alpha$ to the input disturbance δM_F, and is thus the required transfer functiou of the feedforward controller.

Equations (43), (44) and (45) transform to the following (with some rearrangement):

$$(C_1+s)d\mu_{A0}(s)=(C_2\bar{A}+C_3P_0)d\alpha(s)e^{-sT_3}$$
$$-C_2\bar{R}dM_F(s)e^{-sT_1} \quad (46)$$

$$-C_4d\mu_{A0}(s)+C_5d\mu_{A_2}(s)=(C_6\bar{A}+C_3P_1)d\alpha(s)e^{-sT_3}$$
$$-C_6\bar{R}dM_F(s)e^{-sT_1} \quad (47)$$

$$(C_8+s)d\mu_{A_2}(s)=(C_9\bar{A}+C_3P_2)d\alpha(s)e^{-sT_3}$$
$$-C_9\bar{R}dM_F(s)e^{-sT_1} \quad (48)$$

Substitute from Equations (46) and (48) into equations (47) to eliminate $d\mu_{A0}$ and $d\mu_{A_2}$, yielding:

$$\frac{d\alpha(s)}{dM_F(s)}=e^{-s(T_1-T_3)}K\frac{s^2+Ws+X}{s^2+Ys+Z} \quad (49)$$

For the case where α alone is changed:

$$K=\frac{C_6\bar{R}}{C_6\bar{A}+C_3P_1}=3.4570$$

$$W=C_1+C_8+\frac{C_4C_2}{C_6}-\frac{C_5C_9}{C_5}=8.5371$$

$$X=C_1C_8+\frac{C_4C_2C_8}{C_6}-\frac{C_1C_5C_9}{C_6}=18.3341$$

$$Y=C_1+C_8+\frac{C_4(C_2\bar{A}+C_3P_0)}{C_6\bar{A}+C_3P_1}-\frac{C_5(C_9\bar{A}+C_3P_2)}{C_6\bar{A}+C_3P_1}$$
$$=7.3239$$

$$Z=C_1C_8+\frac{C_4C_8(C_2\bar{A}+C_3P_0)}{C_6\bar{A}+C_3P_1}-\frac{C_1C_5(C_9\bar{A}+C_3P_2)}{C_6\bar{A}+C_3P_1}$$
$$=13.6083$$

For the case where both α and r are manipulated in response to δM_F, the same coefficients must be recalculated using Q_0, Q_1 and Q_2 of Equations (39) in place of P_0, P_1 and P_2, respectively, of Equations (38). Thus for changing α with r:

$$K=9.1824$$
$$W=8.5371$$
$$X=18.3341$$
$$Y=6.1065$$
$$Z=9.0260$$

The feedforward controller transfer function was modelled by analog computer and was plugged into the plant analog program at the necessary points.

5.2. Comparison of Plant Responses-Controlled and Uncontrolled.

The simulated granulation plant was subjected to a step increase in feed rate M_F of 1% and the responses of the three variables $\Delta\mu_{G0}$, $\Delta\mu_{G_1}$ and $\Delta\mu_{G_2}$ were automatically plotted. Three runs were made, the first without the feedforward controller operating, the second with the controller operating in Mode α (i. e., manipulating α alone) and the third with the controller operating in Mode αr (i. e., manipulating α together with r). The three sets of plots are given in Fig. 12.

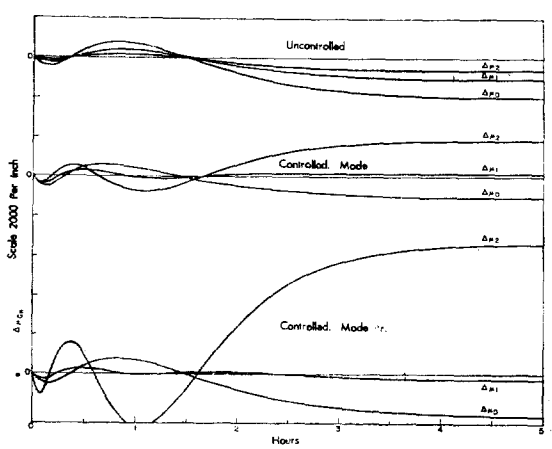

Fig. 12. Response of Granulation Plant to Feed Disturbances.

The fluctuations seen in all the curves up to time 2 hours must be disregarded. They are caused by the inaccuracy of the first-order Padé approximation for

a delay. Thereafter, all curves rise or fall monotonically. The uncontrolled deviation in μ_{G_1} is clearly greatly reduced by both control modes. At the same time, the responses in $\Delta\mu_{G_0}$ and $\Delta\mu_{G_2}$ are somewhat adversely affected, so that the "spread" between the three response curves has been widened. This effect is much more strongly marked in the Mode αr case than in the Mode α, and must be ascribed to the fact that the controller gain in Mode αr is over 2-1/2 times the Mode α gain.

However, the feedforward controller was designed to maintain μ_{G_1} constant, and this has been achieved by both modes of control, manipulating the product recycle fraction α alone, and manipulating α together with crusher speed r according to the relationship of the steady-state operating line.

Because of the large time scale factor, the analog simulation included some small pot settings and amplifier gains. This could only result in some loss of accuracy in computation.

The dynamic plant behavior demonstrated here is sluggish and stable. Theoretically, a closed process loop containing dynamic components and delay components could be inherently oscillatory. In this case, the analog simulation of the plant did not have a closed loop, because cartain terms were too small to be handled on the analog computer. The recorded responses were therefore those of a "straight-through" process.

A suggested feedforward control scheme is indicated in the flow diagram, Fig. 3. Referring to the figure, the total product size flow leaving the sieve is measured by Mass Flow Sensor 1, and that of the product size recycle by Mass Flow Sensor 2. Signals from Sensors 1 and 2 are fed to the "α" Controller 3, which sends a signal to the product recycle feeder controlling the feed rate in order to maintain α at a pre-set value. Crusher speed is maintained by Speed Controller 4.

A change in the P_2O_5 feed rate is sensed by Sensor 5, which sends a signal to Feedforward Controller 6. The latter then sends out a feedforward signal which re-sets the control points of Controllers 3 and 4.

6. Conclusions

It was demonstrated that the linearized model of the plant was a good representation of the original nonlinear model, in terms of dynamic response. Thereafter, the linearized model alone was used. It was also found that the process, as simulated, was effectively a "straight-through" one rather than closed loop. Both of these facts made the design and operation of a feedforward controller for keeping average particle size constant a straight-forward matter.

It has been shown that it is normally desirable to vary product recycle fraction α in conjunction with crusher speed r, in order to maintain the granulation discharge particle size distribution unchanged. In spite of this, it was shown that, because of the smaller controller gain required, it was better to offset feed disturbances by manipulating α alone. Presumably, after a new steady-state has been reached, the crusher speed can be adjusted to suit.

If the granulator model had given rise to larger deviations in the output variables in response to disturances, the "process feedback" terms (see Equations (31) and (32)) would not have been negligible, and the process would have been effectively a closed-loop one. Unfortunately no dynamic plant data was available to check this point.

Acknowledgement

The authors wish to express their warmest thanks to Mr. T. P. Hignett of the Tennessee Valley Authority at Muscle Shoals, Alabama, for permission to use their Diammonium Phosphate Pilot Plant data in this study. Our thanks, also, to Mr. Charles H. Davis of the same organization, for providing the material.

Warm thanks are due, in addition, to the American Cyanamid Company, whose donation of analog computer facilities to the Department of Chemical Engineering at the Polytechnic Institute of Brooklyn made this work possible.

Nomenclature

Latin Letters

$\bar{A}$ Coefficient for computing ΔR for $\delta\alpha$.

C Coefficients of linearized ammoniator equations. Analog program.

D Particle size.

D_1 Smallest particle size.

D_2 Lower sieve opening.

D_3 Upper sieve opening.

D_4 Largest particle size.

f Particle size distribution function. Thus:

$$f(D)dD = \frac{\text{no. of Particles of size between } D \text{ and } (D+dD)}{\text{unit mass of stream}}$$

M Mass flow rate of a particle stream.

$\bar{M}$ Steady-state mass flow rate.

N Particle flow rate of a particle stream.

n Number of particles per unit mass of a particle stream.

P Coefficient for computing $\Delta\mu_R$ from $\delta\alpha$. (α alone).

Q Coefficient for computing $\Delta\mu_R$ from $\delta\alpha$. (α with r).

R Overall recycle ratio.

$\bar{R}$ Steady-state recycle ratio.

r Crusher speed.

$\bar{r}$ Steady-state crusher speed.

s Laplace transform variable.

T Generalized time delay.

T_1 Preneutralized time delay.

T_2 Dryer time delay.

T_3 Transport time delay.

t Time.

W, X, Y, Z Coefficients in feedforward controller trasfer function.

Greek Letters

α Fraction of product size material recycled.

$\bar{\alpha}$ Steady-state α.

ε Particle growth rate.

μ Moment of unnormalized particle size distribution.

$\bar{\mu}$ Steady-state μ.

ν Particle volume shape factor.

ρ Density of particle material.

Φ Granulator hold-up

$\bar{\Phi}$ Steady-state Φ.

τ Residence time in granulator. Random variable of residence time. Analog program scaled time variable.

Deviation Variables(Typical)

ΔR Deviation in R, where: $R^*=\bar{R}+\Delta R$.

$\delta\alpha$ Fraction deviation in 2, where: $\alpha^*=\bar{\alpha}(1+\delta\alpha)$.

Subscripts

A Ammoniator outlet stream.

C Crusher discharge stream.

F Feed stream.

G Granulator discharge stream.

i Number index, coefficients.

n Number index, distribution moments.

O Oversize fraction.

P Product size fraction.

R Recycle stream.

U Undersize fraction.

X Recycle stream prior to transport delay.

References

(1) Bollinger, R. E. and Lamb, D. E.; *I. & E. C.* Fundamentals, **1**, 245 (1962).

(2) Han, C. D. and Wilenitz, I.; *I, & E. C.* Fundamentals, **9**, 401 (1970).

(3) Horn, W. R. and Fouser, N. D.; Chemical Engineering Progress, **62**, 109 (1966).

(4) Report on Pilot Plant Demonstrations of the Production of Granular Fertilizers, TVA, 1959.

(5) Sauchelli, V.; "Chemistry & Technology of Fertilizers," Reinhold, New York, 1960.

(6) Wilenitz, I., Ph. D. Thesis (*Ch. E.*), Polytechnic Institute of Brooklyn, June, 1970.

(7) Young, R. D., Hicks, G. C. and Davis, C. H.; Agricultural and Food Chemistry, **10**, 442 (1962).